Silver halide IR fibre with extra small diameter

E.A. Korsakova[1], N.A. Muftahitdinova[1], I.A. Kashuba[1], A.S. Korsakov[1], L.V. Zhukova[1]

[1]Ural Federal University named after the first President of Russia B.N. Yeltsin, Mira st. 19, Yekaterinburg, Russia, 620002

Abstract. We developed fine extrusion dies and accessories for implementing the direct high-temperature extrusion. It allowed us to fabricate a silver halide polycrystalline single-layer fibre of a new miniaturization level. This fibre has a diameter of 110 μm (the previous minimum diameter was 300 μm). We measured the fibre's optical properties, such as refractive index dispersion, transmission range, optical losses including bending losses, mode field distribution of CO_2 laser radiation at 10.6 μm (in the far field). We also estimated the roughness of the fibre lateral surface and the ellipticity of the fibre end faces. It was found that 110 μm fibre is highly transparent in the wavelength range of 2-20 μm and has low bending losses. It has rather smooth surface, the almost perfect circle cross-section and the small deviation of the nominal diameter along the fibre. These fibres, assembled in mechanical fibre bundles, may be useful for IR imaging, IR spectroscopy, and IR microscopy. They also may be used as billets of inserts for various PCFs and fibre bundles with common background cladding (matrix) with improved functional characteristics.

1. Introduction

Aimed at miniaturization, the middle infrared optics (from 2 to 50 μm), in particular, MIR fibre optics has been significantly advanced for recent years. This allowed extending the scope of application of MIR fibres in high-resolution imaging systems for a variety of scientific, industrial and medical applications, including industrial remote inspection systems and medical endoscopes [1, 2].

Among MIR fibres, the largest part of this range is covered by polycrystalline silver halide fibres. They are highly transparent in the spectral range from 2.5 to 20 μm without absorption windows. Some compositions of the fibres (such as silver halides doped with thallium (I)) allow them to transmit radiation up to 25 μm. Silver halide fibres are non-toxic, non-hygroscopic and not affected by recrystallization. Photosensitivity is one of their disadvantages, although solid solutions of AgCl–AgBr system are resistant to visible and infrared radiation unlike AgCl and AgBr individual crystals [3]. Until recently, however, the smallest diameter of the polycrystalline silver halide fibres was no less than 300 μm [4], while a fibre diameter reduction would be crucial for many applications. In this paper, we demonstrate a possible way of the size diminution for the fibres based on silver halides.

2. Materials

We used the Bridgman technique to grow $AgCl_{0.25}Br_{0.75}$ high purity single crystals [5]. This composition corresponds to the composition of the phase diagram minimum point. Therefore, it does not vary along the crystal that is good for maintaining desired properties.

Then we measured the refractive index dispersion for this material. As samples, we used polycrystalline plates obtained from the single crystals. The crystals were treated mechanically and hot

embossed using the Specac 15 Ton hand hydraulic press at the temperature of 120 ^{o}C and the pressure of 6 t [6]. The thickness of the obtained plates was measured with a mechanical hand micrometer of the MC-25 type. After cooling these plane-parallel plates to room temperature, we recorded their transmission spectra up to 20 μm using an IR-Fourier spectrophotometer (FTIR) IR Prestige-21. For finding refractive indices in the MIR range we used interference spectra [7]. We also recorded ultraviolet–near infrared spectra of the samples within the range of 190–1100 nm with the help of a Shimadzu UV-1800 spectrophotometer. To measure the refractive index in this range we used the method, described in the paper [8]. The overall results are shown in figure 1.
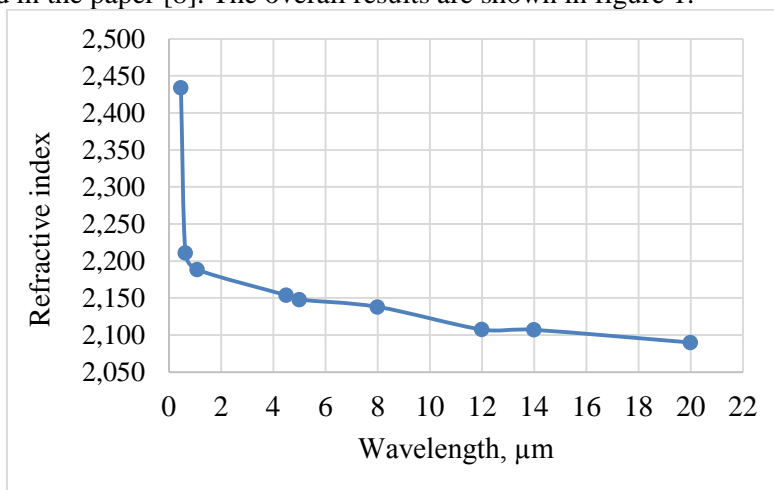

Figure 1. Refractive index dispersion of $AgCl_{0.25}Br_{0.75}$ crystals.

As seen from the graph x, the refractive index is descending monotonically, but nonlinearly, within the composition. General behaviour resembles that of common covalent and ionic optical materials, including I-VII ionic crystals, which proves the absence of refractive index anomalies within the concerned wavelength range [9].
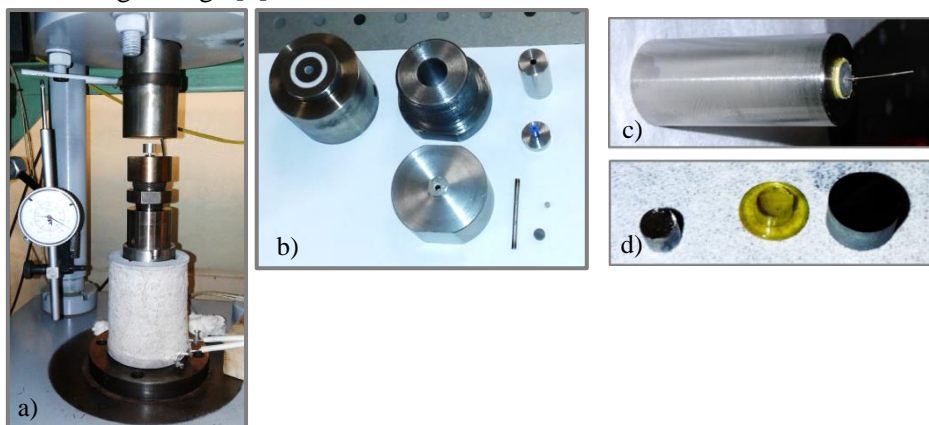

Figure 2. Extrusion die and accessories: (a) the appearance of extrusion container in working position, (b) equipment for the extrusion of fibres with Ø 110 μm, (c) container and die with extrusion discard, (d) extrusion plug, $AgCl_{0.25}Br_{0.75}$ discard and die.

3. Fibre fabrication

Silver halide crystals have good plasticity and demonstrate no cleavage. Therefore they can be used to produce polycrystalline IR fibres by extruding [10]. We developed fine extrusion dies and accessories for implementing direct high-temperature extrusion in order to gain the fibre of 110 μm in diameter (see figure 2 a, b). The obtained $AgCl_{0.25}Br_{0.75}$ single crystal was turned to form a small cylindrical billet of 3 mm in diameter and 6 mm in height. Then, a polycrystalline single-layer fibre was fabricated using the developed accessories for the extrusion at a temperature of 450 K and pressure of

500 MPa. We used 2 stage extrusion as shown in figure 3. As seen in figure 2 c, d, an extrusion discard is rather thin that indicates the good alignment of the setup. After the extrusion, the fibre was contained into a shell made of PEEK tube and their end faces were carefully polished.
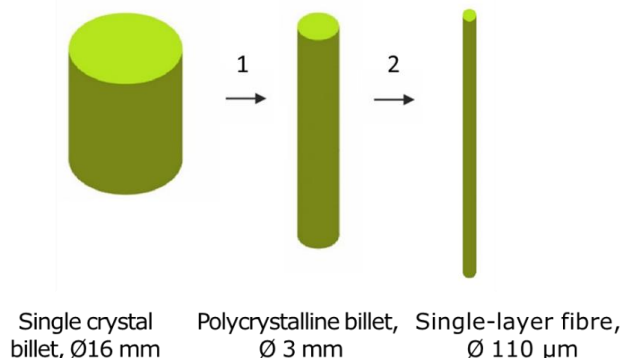

Single crystal billet, Ø16 mm   Polycrystalline billet, Ø 3 mm   Single-layer fibre, Ø 110 µm

Figure 3. Scheme of 2 stage extrusion of 110 µm single-layer fibre based on silver halides.

4. Fibre characterization

The overall dimensions of the fibre obtained are as follows: the length is 2.5 m, and the diameter varies from 110 to 111 µm. Thus, the size variation doesn't exceed 0.45 % along the fibre. This deviation may be attributed to the measurement error. The appearance of the fibre is shown in figure 4.
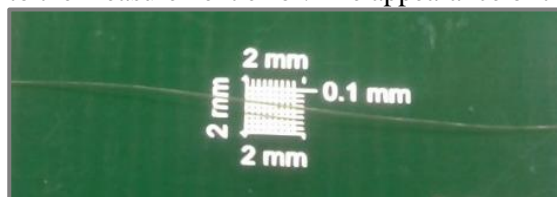

Figure 4. Photo of 110 µm $AgCl_{0.25}Br_{0.75}$ single-layer fibre.

The quality of the fibre lateral surface was visually assessed using a microvisor LOMO vizo-MET-221 (see figure 5). Micrographs showed that the surface roughness is several times smaller than the transmitted wavelengths, which is very important for minimizing optical losses due to surface scattering [11].
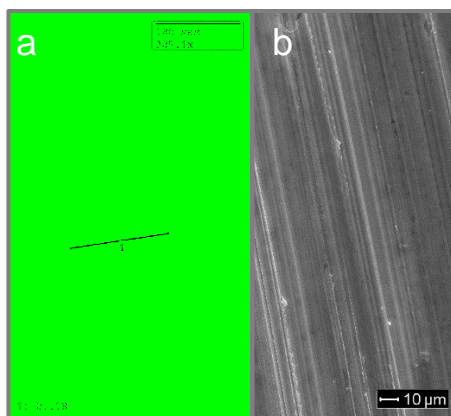

Figure 5. Micrographs of the lateral fibre surface: (a) X20 magnification; (b) the same, but X50 magnification.

Structure defects of the fibre lateral surface were studied using a scanning electron microscope FEI CM 30. It was found that the surface does not contain large cavities and the average surface grain size is 120 nm (see figure 6).

Moreover, we checked the ellipticity of the fibre end cross section. It was found that longitudinal and transverse sizes are the same, in considered case 111 µm (see figure 7 a and b).
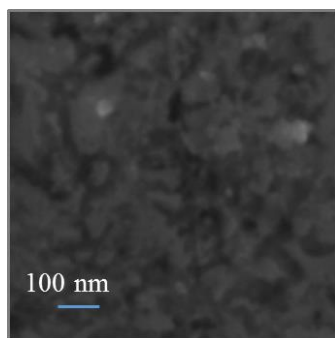
Figure 6. SEM image of the fibre lateral surface; average grain size is 120 nm.
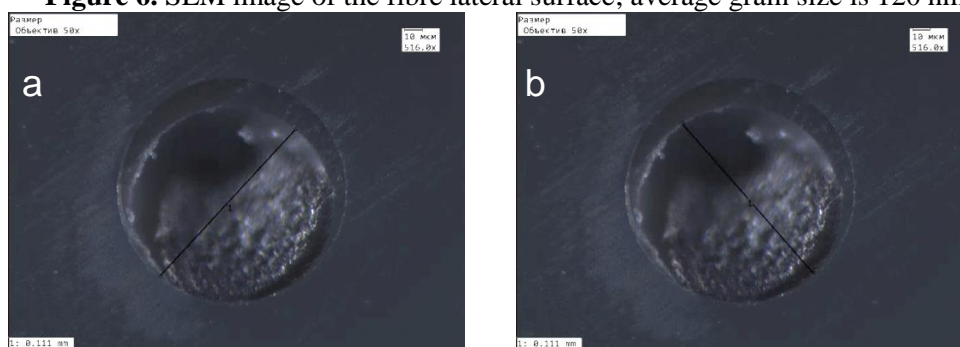

Figure 7. Micrographs of the fibre end cross section: (a) longitudinal size; (b) transverse size.

IR transmission spectrum of the fibre was registered using a Shimadzu FTIR spectrometer IR Prestige-21. The measurement was carried out through the full fibre length. The recording conditions were as follows: the beam divider – KBr, the detector – mercury cadmium telluride (MCT) detector, the wavelength range – 5000–500 cm^{-1}, resolution – 4 cm^{-1}. We used an attachment with parabolic off-axis mirrors to introduce infrared radiation into the fibre under investigation. To obtain spectrum, an auxiliary fibre was first used, and the spectrum obtained for the test fibre was set as the background. Then the fibre under investigation was connected to the auxiliary fibre and the final spectrum was registered (see figure 8). This technique allowed us to determine the transparency of IR fibres in percentages and eliminate the atmospheric background that was not possible in the first technique. As seen in figure 8, the fibre is transparent in the range from 2 to 20 μm, which is the typical transmission range for silver halide fibres.
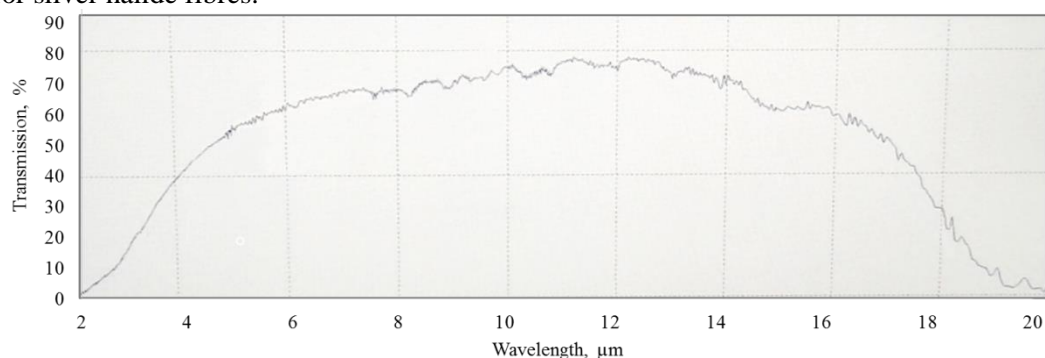

Figure 8. Transmission spectrum of $AgCl_{0.25}Br_{0.75}$ fibre of 110 μm in diameter.

The far-field distribution of CO_2 laser radiation ($\lambda = 10.6$ μm) at the output fibre end was assessed using the setup shown in figure 9. It consisted of a CO_2 laser Synrad 48 Series M 10 Wt ($\lambda = 10.6$ μm), a laser power and energy meter OPHIR Vega, two ZnSe lenses with the focal distance of 50 mm, and a pyroelectric camera Spiricon Pyrocam III. We observed a typical multimode working regime without focusing the output radiation (see figure 10 a). When we focused the outgoing radiation by means of ZnSe lens (F = 50 mm), a Gaussian-like distribution was observed (see figure 10 b).
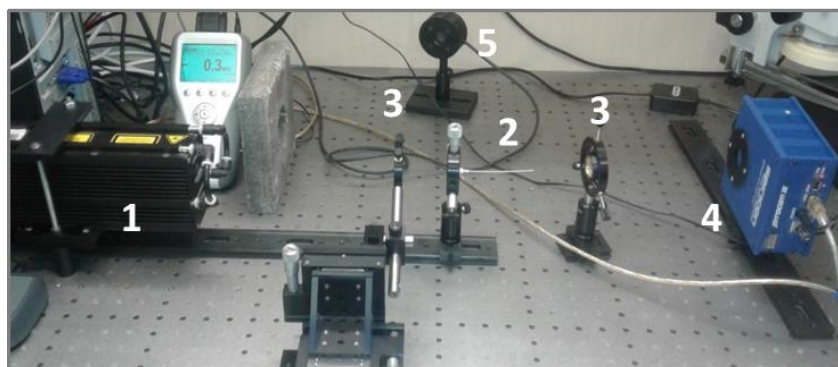
Figure 9. Setup for measuring optical losses and far-field study of output beam profile: 1 – CO_2 laser; 2 – fibre Ø 110 μm; 3 – ZnSe lenses; 4 – CCD camera; 5 – thermal head.
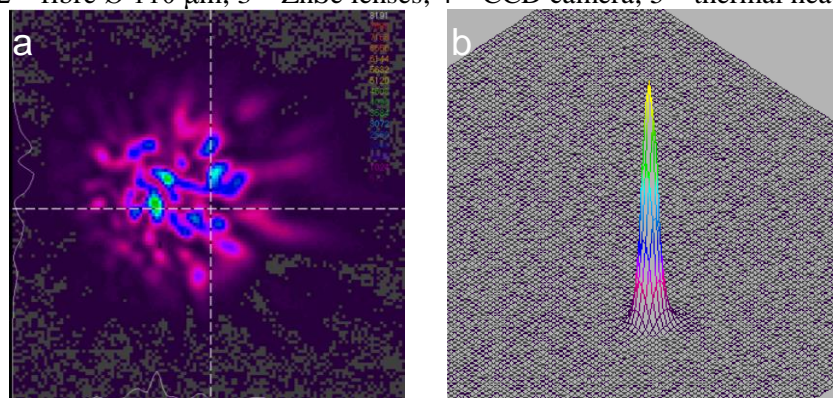

Figure 10. Far-field distribution of CO_2 laser radiation (@ 10.6 μm) transmitted through Ø 110 μm fibre: (a) without focusing (b) with focusing by ZnSe lens.

Optical losses (the attenuation coefficient) were measured by the cut-back technique using the setup shown in figure 9 as well. According to this technique, at the first stage, we measured the transmission of the full-length fibre. Then, we cut off a short segment of the fibre and measured its transmission. The attenuation of the fibre at 10.6 μm was calculated with the expression:

$$\alpha = \frac{10 \lg(P_2/P_1)}{(l_2 - l_1)},$$ (1)

where P_2 and P_1 are the values of the laser power (mW) measured at the output ends of the fibre of full-length l_2 and the cut-off fibre of length l_1, respectively. The cut-back technique allows eliminating the Fresnel reflections from the fibre end faces, which are cancelled out in Eq. (1) [12]. In this case, it is assumed that the attenuation coefficient along the fibre is constant. It was found, that the attenuation of Ø 110 μm fibre is 0.4 dB/m.

One of the main characteristics of optical fibres is their flexibility [13]. It is important to ensure that bending does not affect the transmission up to some acceptable values of curvature. For measuring the power transmission of the bent fibre, we used an experimental setup which is shown in figure 11. A CO_2 laser beam was focused onto the fibre using a ZnSe lens. The proximal fibre end was in a fixed position. The distal fibre end could be displaced to bend the fibre. The fibre was bent around two cylinders of a given bending radius R. The distal end of the bundle was directed at a power detector (Ophir). Bending losses were measured at the curvature angle of 50°. The power measurements were carried out for bending radii of 2, 3, 4, and 5 cm. The results, plotted relative to the power transmitted by a straight bundle, are shown in figure 12. As seen from the figure, there is no substantial power loss in the fibre for all considered radii of curvature.

It is worth to be mentioned that all measurements were carried out while the fibre was contained into a PEEK tube. Figure 13 demonstrates a photo of the possible fibre curvature without a shell.
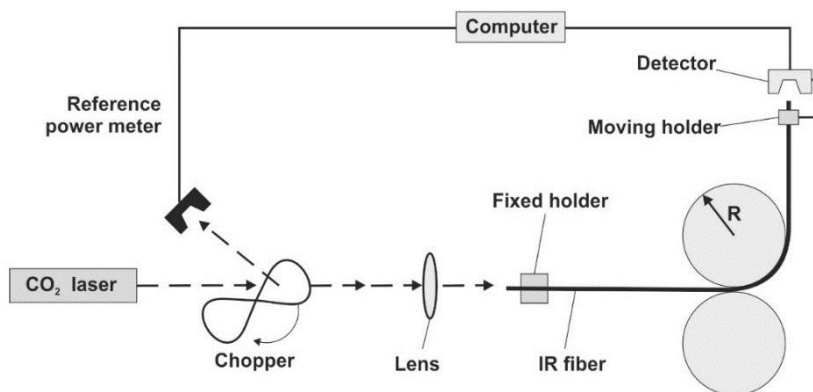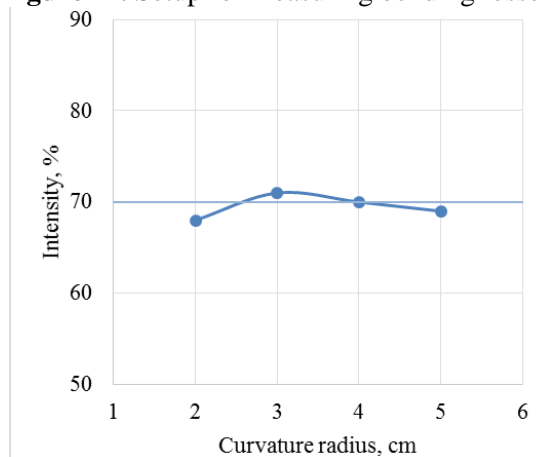
Figure 11. Setup for measuring bending losses.

Figure 12. Intensity of radiation transmitted through the bent fibre at various radii of curvature.

Figure 13. Example of possible curvature of the fibre with 110 µm in diameter (without shell).

5. Conclusion

We developed fine extrusion dies and accessories for implementing direct high-temperature extrusion. It allowed fabricating a pioneer single-layer infrared fibre of $AgCl_{0.25}Br_{0.75}$ solid solution crystal. This fibre has a diameter of 110 with the deviation from the nominal value of 0.45 % and the length of 2.5 m. It is transparent in the wavelength range from 2 to 20 µm. The refractive index of the material varies from 2.175 to 2.090 within the transmission range. We also estimated the roughness of the fibre lateral surface and it was found that the fibre has the rather smooth surface. The attenuation of the silver halide fibre is 0.4 dB/m and bending losses are negligible for the curvature radii down to 2 cm. These fibres, assembled in mechanical fibre bundles, may be useful for IR imaging, IR spectroscopy, and IR microscopy in many scientific, industrial and medical applications. They also may be used as billets of inserts for various improved PCFs [14] and fibre bundles with common background cladding.

6. References

[1]   Tofail, S.A.M. In Situ, Real-Time Infrared (IR) Imaging for Metrology in Advanced Manufacturing / S.A.M. Tofail, A.A. Mani, J. Bauer, C. Silien // Adv. Eng. Mater. – 2018. – Vol. 20. – P. 1800061. DOI: 10.1002/adem.201800061.

[2]   Gopal, V. Coherent hollow-core waveguide bundles for infrared imagning / V. Gopal, J.A. Harrington, A. Goren, I. Gannot // Optical Engineering. – 2004. – Vol. 43. – P. 1195-1199. DOI: 10.1117/1.1687729.

[3]   Korsakov, A.S. Investigating the light stability of solid-solution-based AgCl-AgBr and AgBr-TlI crystals / A.S. Korsakov, A.E. Lvov, D.S. Vrublevsky, L.V. Zhukova // Chinese Optics Letters. – 2016. – Vol. 14. – P. 020603. DOI: 10.3788/COL201614.020603.

[4]   Polycrystalline IR-Fibres: specifications [Electronic resource]. – Access mode: https://artphotonics.com/product/polycrystalline-ir-fibres/ (accessed 29.11.2018).

[5]   Korsakov, A.S. Structure modeling and growing $AgCl_xBr_{1-x}$, $Ag_{1-x}Tl_xBr_{1-x}I_x$, and $Ag_{1-x}Tl_xCl_yI_zBr_{1-y-z}$ crystals for infrared fiber optics / A.S. Korsakov, L.V. Zhukova, E.A. Korsakova, E.V. Zharikov // J. Cryst. Growth. – 2014. – Vol. 386. – P. 94-99. DOI: 10.1016/j.jcrysgro.2013.09.045.

[6]   Korsakov, A.S. Investigating the optical properties of polycrystalline AgCl(1-x)Br(x) ($0 \leq x \leq 1$) and Ag(0.95)Tl(0.05)Br(0.95)I(0.05) for IR engineering // A.S. Korsakov, D.S. Vrublevsky, V.S. Korsakov, L.V. Zhukova // Appl. Opt. – 2015. – Vol. 54. – P. 8004-8009. DOI: 10.1364/AO.54.008004.

[7]   Korsakov, A.S. Refractive index dispersion of $AgCl_{1-x}Br_x$ ($0<x<1$) and $Ag_{1-x}Tl_xBr_{1-x}I_x$ ($0<x<0.05$) // A.S. Korsakov, D.S. Vrublevsky, A.E. Lvov, L.V. Zhukova // Opt. Mater. – 2017. – Vol. 64. – P. 40-46. DOI: 10.1016/j.optmat.2016.11.038.

[8]   Padera, F. Measuring Absorptance (k) and Refractive Index (n) of Thin Films with the PerkinElmer Lambda 950/1050 High Performance UV-Vis/NIR Spectrometers // Application note: UV/Vis Spectroscopy. – CT USA: Shelton, 2013. – 9 p.

[9]   Voronkova, E. Optical Materials for the Infrared Engineering / E. Voronkova, B. Gretchushnikov, G. Distler, I. Petrov. – Moscow: Nauka, 1963. – 336 p.

[10]   Zhukova, L.V. $AgCl_xBr_{1-x}$ and $AgCl_xBr_yI_{1-x-y}$ crystals for IR engineering and optical fiber cables / L.V. Zhukova, N.V. Primerov, A.S. Korsakov, A.I. Chazov // Inorg. Mater. – 2008. – Vol. 44. – P. 1372-1377.

[11]   Israeli, S. Influence of the surface roughness of silver halide fibers on their transmission in the near infrared / S. Israeli, A. Katzir // Opt. Mater. – 2012. – Vol. 34(9). – P. 1579-1587. DOI: 10.1016/j.optmat.2012.03.037.

[12]   Israeli, S. Attenuation, absorption, and scattering in silver halide crystals and fibers in the midinfrared / S. Israeli, A. Katzir // J. Appl. Phys. – 2014. – Vol. 115. – P. 023104.

[13]   Lavi, Y. Flexible ordered bundles of infrared transmitting silver-halide fibers: design, fabrication, and optical measurements / Y. Lavi, A. Millo, A. Katzir // Appl. Opt. – 2006. – Vol. 45(23). – P. 5808-5814.

[14]   Korsakov, A.S. Investigating the properties of infrared PCFs based on AgCl-AgBr, AgBr-TlI, AgCl-AgBr-AgI(TlI) crystals theoretically and experimentally / A.S. Korsakov, L.V. Zhukova, D.S. Vrublevsky, E.A. Korsakova // Opt. Spectrosc. – 2014. – Vol. 117(6). – P. 960-963.